**SUPPLEMENTARY INFORMATION**

# Figure S1

## A

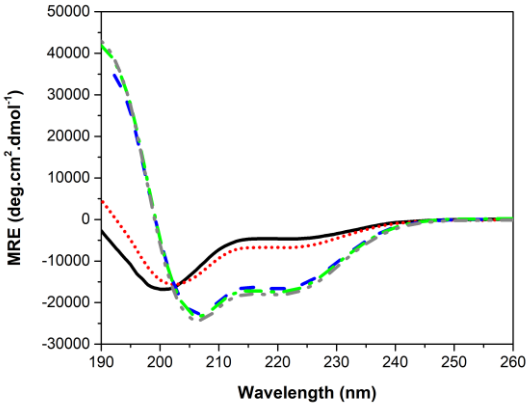


| % TFE | % Helix |
|---|---|
| 0 | 14 |
| 10 | 20 |
| 25 | 48 |
| 50 | 50 |
| 75 | 52 |

## B

**DrugScore PPI Analysis of CDK4**

| Residue | ΔΔG (Kcal/mol) | Residue | ΔΔG (Kcal/mol) | Residue | ΔΔG (Kcal/mol) |
|---|---|---|---|---|---|
| $G_{48}$ | ≤ 0 | $R_{55}$ | 0.59 | $R_{62}$ | 0.34 |
| $L_{49}$ | 1.42 | $E_{56}$ | ≤ 0 | $L_{63}$ | ≤ 0 |
| $P_{50}$ | ≤ 0 | $V_{57}$ | 0.65 | $E_{64}$ | 0.22 |
| $I_{51}$ | 1.07 | $A_{58}$ | ≤ 0 | $A_{65}$ | ≤ 0 |
| $S_{52}$ | ≤ 0 | $L_{59}$ | 0.21 | $F_{66}$ | 0.23 |
| $T_{53}$ | 0.11 | $L_{60}$ | ≤ 0 | $E_{67}$ | 0.24 |
| $V_{54}$ | 1.04 | $R_{61}$ | 1.04 | | |

Computational alanine scanning (Drugscore PPI) of the C-helix of CDK4 ($G_{48}L_{49}P_{50}I_{51}S_{52}T_{53}V_{54}R_{55}E_{56}V_{57}A_{58}L_{59}L_{60}R_{61}R_{62}L_{63}E_{64}A_{65}F_{66}E_{67}$ ) in interaction with cyclin D1 (PDB: 2W9Z). Free energy binding differences ($\Delta\Delta G$) for wildtype residue-to-Ala mutations. Positive free energy binding differences indicate a potential hot spot residue. In red $\Delta\Delta G$ >0.5 Kcal/mol, in green $\Delta\Delta G \leq 0$.

**FIGURE S1 –**

**(A) Tendency of the peptide derived from CDK4 C helix to adopt a helical conformation**

100 µM CDK4-Chelix peptide in NaP 50 mM, pH 7.0, 20°C displays a random conformation, whilst TFE induces helicity, with a maximum achieved with 25% TFE, indicating its propensity to form a helix in the appropriate environment. Overlay of far-UV CD spectra of CDK4-Chelix peptide short alone (black line) and in presence of 2,2,2-Trifluoroethanol (TFE), 10 % TFE (red dots), 25 % (blue dashed line), 50 % (green dashed-dotted line) and 75 % (grey dashed-dot-dot).

**(B)** Computational alanine scanning (Drugscore PPI) of the C-helix of CDK4 ($G_{48}L_{49}P_{50}I_{51}S_{52}T_{53}V_{54}R_{55}E_{56}V_{57}A_{58}L_{59}L_{60}R_{61}R_{62}L_{63}E_{64}A_{65}F_{66}E_{67}$ ) in interaction with cyclin D1 (PDB: 2W9Z). Free energy binding differences ($\Delta\Delta G$) for wildtype residue-to-Ala mutations. Positive free energy binding differences indicate a potential hot spot residue. In red $\Delta\Delta G$ >0.5 Kcal/mol, in green $\Delta\Delta G \leq 0$.

## Figure S2

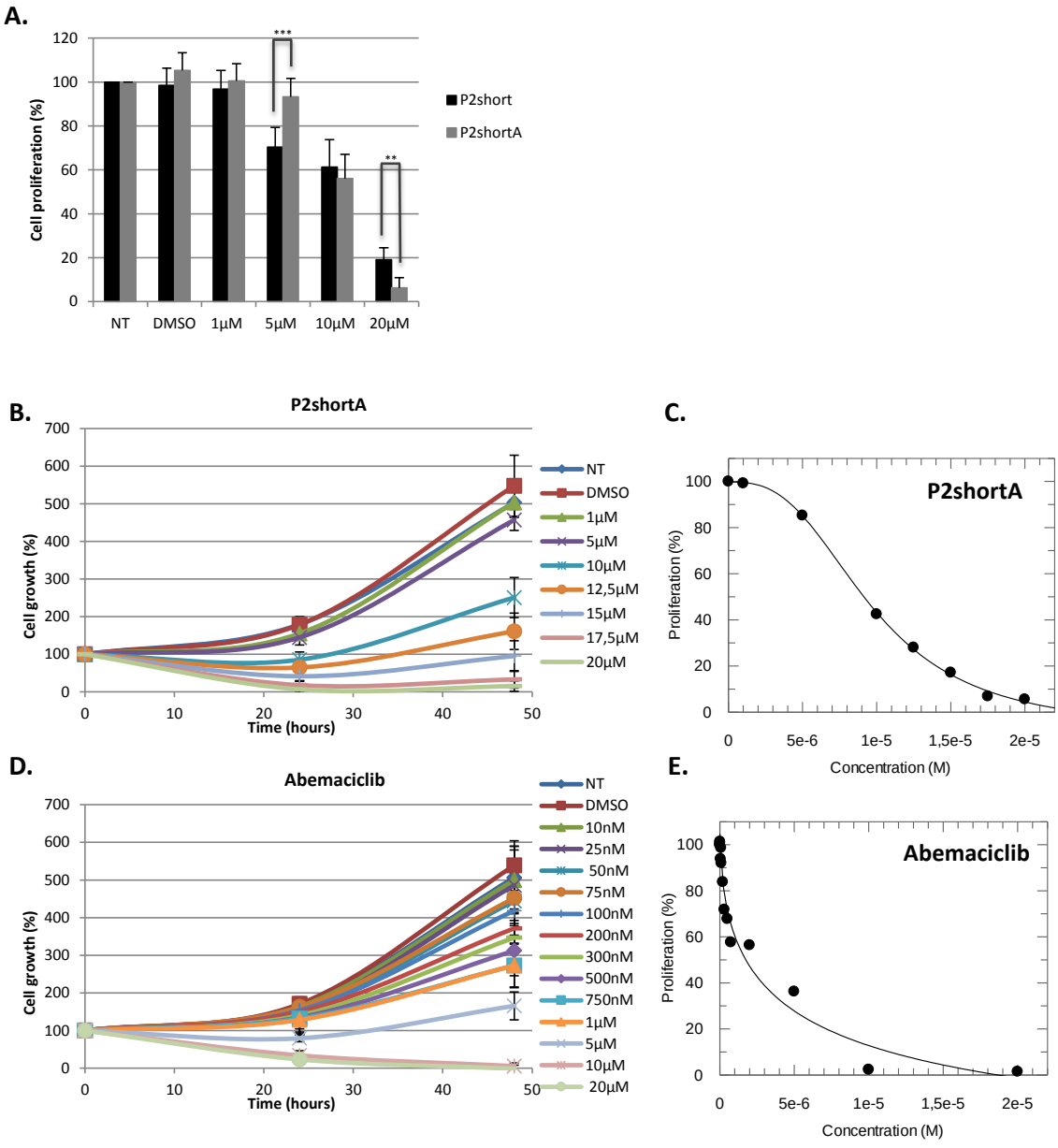


**FIGURE S2– Proliferation assays and determination of IC50s**

Proliferation assays were performed by crystal violet staining every 24 hours.

**(A)** A549 cells were exposed to different concentrations of P2short and P2shortA peptides during 48 hours. Results are presented as average of nine independent experiments (n=4/experiment) ± SD. Means were compared with t test, * p<0,01, ** p<0,001, *** p<0,0001.

**(B-G)** A549 cells were treated with different concentrations of P2shortA (B,C) or Abemaciclib (D,E) for 48 hours. Curves represented means of at least two independent experiments (n=4/experiment) ± SD. $IC_{50}$ were determined with Grafit software.

## Figure S3

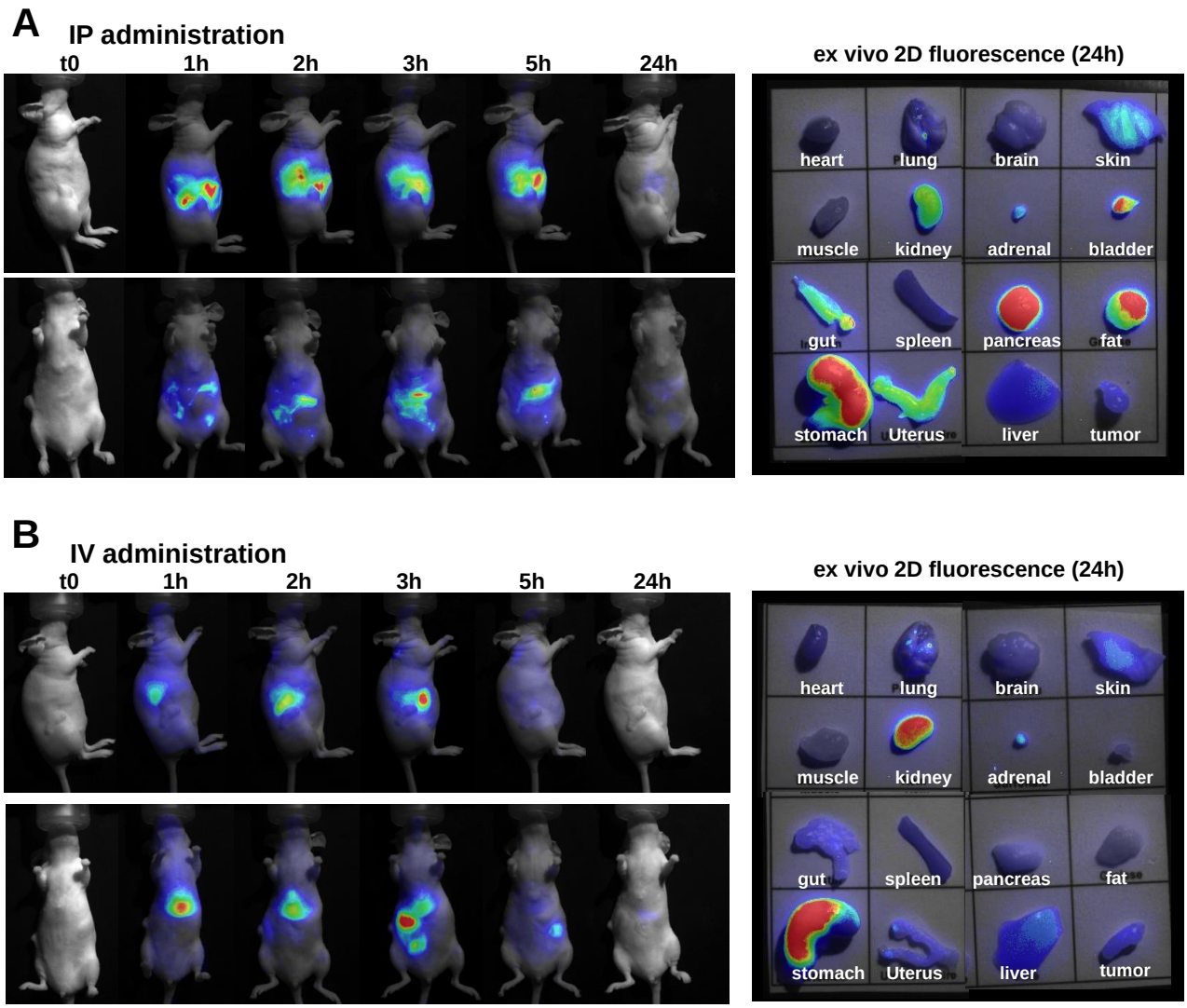
A
IP administration
t0
1h
2h
3h
5h
24h
ex vivo 2D fluorescence (24h)
heart
lung
brain
skin
muscle
kidney
adrenal
bladder
gut
spleen
pancreas
fat
stomach
Uterus
liver
tumor
B
IV administration
t0
1h
2h
3h
5h
24h
ex vivo 2D fluorescence (24h)
heart
lung
brain
skin
muscle
kidney
adrenal
bladder
gut
spleen
pancreas
fat
stomach
Uterus
liver
tumor
C
control
P2-shortA IP
P2-shortA IV 5h
P2-shortA IV 24h
RLU/pixel/100 ms
60000
40000
20000
0
Heart
Uterus
Brain
Gut
Adrenal
Muscle
Kidney
Spleen
Liver
Pancreas
Fat
Skin
Lung
Tumour

**FIGURE S3 – Cy5.5-P2shortA circulates a few hours in the bloodstream after intravenous administration, but not after intraperitoneal administration, in mice with NSCLC subcutaneous tumour.** 8 µmol.$L^{-1}$ Cy5.5-P2shortA were administered intraperitoneally (IP) or intravenously (IV) in mice with subcutaneous NSCLC A549 or H358 tumour. **(A)** Fluorescence images (20 ms integration time) were recorded at the indicated time after IP injection of Cy5.5-P2-short (min-max: side 4000-23093; frontal 4000-60775). Representative images performed on isolated organs 24h after IP are shown. **(B)** Fluorescence images (20 ms integration time) were recorded at the indicated time after IV injection of Cy5.5-P2-short (min-max: side 2121-40518; frontal 2121-37520). Representative images performed on isolated organs 24h after IV injection are shown. **(C)** Region of interest (ROI) are defined on extracted organs to semi-quantify the amount of photons detected per pixel after a 100 ms exposure. The results in each organ are expressed as the mean ± SD in tumour-bearing mice (IP, n≥2; IV, n=3), or non-injected healthy mouse (control). IP injection showed biodistribution of Cy5.5-P2shortA mainly in the abdomen, whereas IV injection showed biodistribution of Cy5.5-P2shortA in several organs after 5 h and mainly in the kidneys after 24h.

## Figure S4

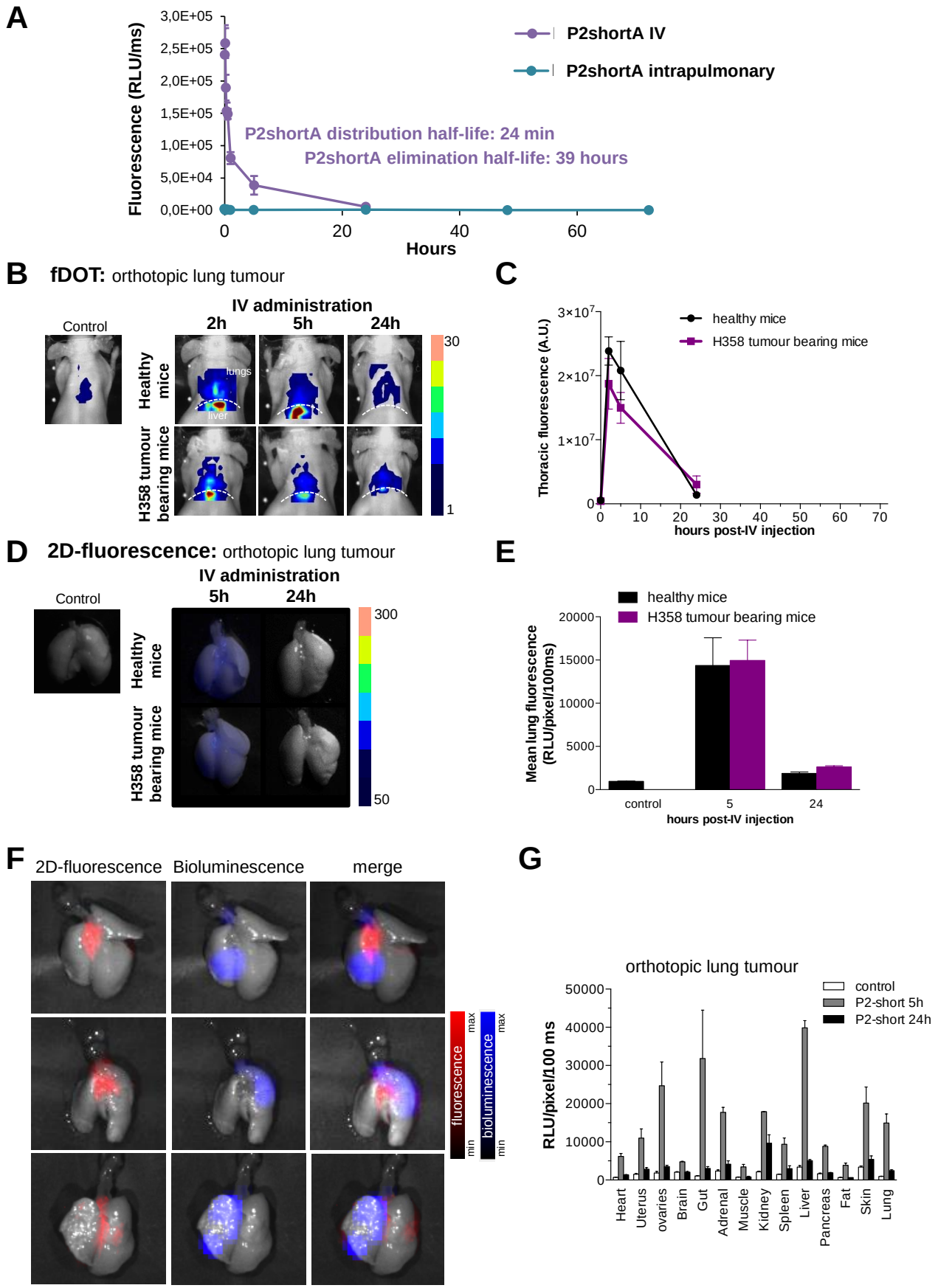
A
Fluorescence (RLU/ms)
3,0E+05
2,5E+05
2,0E+05
1,5E+05
1,0E+05
5,0E+04
0,0E+00
0
20
40
60
Hours
P2shortA IV
P2shortA intrapulmonary
P2shortA distribution half-life: 24 min
P2shortA elimination half-life: 39 hours
B fDOT: orthotopic lung tumour
IV administration
2h
5h
24h
Control
Healthy mice
H358 tumour bearing mice
lungs
liver
30
1
C
Thoracic fluorescence (A.U.)
3×10^7
2×10^7
1×10^7
0
0
10
20
30
40
50
60
70
hours post-IV injection
healthy mice
H358 tumour bearing mice
D 2D-fluorescence: orthotopic lung tumour
IV administration
5h
24h
Control
Healthy mice
H358 tumour bearing mice
300
50
E
Mean lung fluorescence (RLU/pixel/100ms)
20000
15000
10000
5000
0
control
5
24
hours post-IV injection
healthy mice
H358 tumour bearing mice
F
2D-fluorescence
Bioluminescence
merge
fluorescence
bioluminescence
max
min
G
orthotopic lung tumour
RLU/pixel/100 ms
50000
40000
30000
20000
10000
0
control
P2-short 5h
P2-short 24h
Heart
Uterus
ovaries
Brain
Gut
Adrenal
Muscle
Kidney
Spleen
Liver
Pancreas
Fat
Skin
Lung

**FIGURE S4 – Cy5.5-P2shortA circulates in the bloodstream after intravenous injection.**

**(A)** Healthy mice were injected intravenously (200µL) or intrapulmonary (50µL) with 10 µmol.$L^{-1}$ Cy5.5-P2shortA. The fluorescence intensity measurements of blood samples were performed over time. The results are expressed as the mean ± SD (n=6). Intravenous injection showed Cy5.5-P2shortA blood distribution half-life of 24 min and Cy5.5-P2shortA blood elimination half-life of 39h, whereas intrapulmonary administration showed Cy5.5-P2shortA below sensitivity threshold.

**(B-G)** 10 µmol.$L^{-1}$ Cy5.5-P2shortA were administered intravenously (200 µL) in orthotopic H358 tumour-bearing mice. **(B)** 3D-fluorescence tomography imaging (fDOT) was performed at the indicated time after administration of Cy5.5-P2shortA. Dotted line: position of diaphragm. **(C)** Volumes of interest are defined on the thoracic region to semi-quantify the total amount of photons. The results are expressed as the mean ± SEM in healthy (5h, n≥5; 24h, n≥3) or H358 tumour-bearing mice (5h, n≥6; 24h, n≥2). **(D)** Fluorescent images were performed on isolated lungs at the indicated time after Cy5.5-P2shortA injection. **(E)** Regions of interest (ROIs) are defined on the extracted lungs to semi-quantify the amount of photons detected per pixel after a 100 ms exposure. The results are expressed as the mean ± SEM in healthy (n=4), or H358 tumour-bearing lungs (n≥3), or non-injected healthy mouse (control). **(F)** Bioluminescence, and 2D-fluorescence imaging were performed on isolated lungs 5h after intravenous injection of Cy5.5-P2shortA. Bioluminescent signal showed H358-Luc tumour cells in lungs (in blue); 2D-fluorescent signal showed Cy5.5-P2shortA location in the lungs (in red); fluorescent and bioluminescent signals were merge. No colocalization between Cy5.5-P2shortA signal and H358 tumours was observed in lungs after intravenous injection of P2-short. **(G)** ROIs are defined on the organs to semi-quantify the amount of photons detected per pixel after a 100 ms exposure. The results are expressed as the mean ± SEM in healthy (n=4), or H358 tumour-bearing lungs (n≥3), or non-injected healthy mouse (control).

## Figure S5

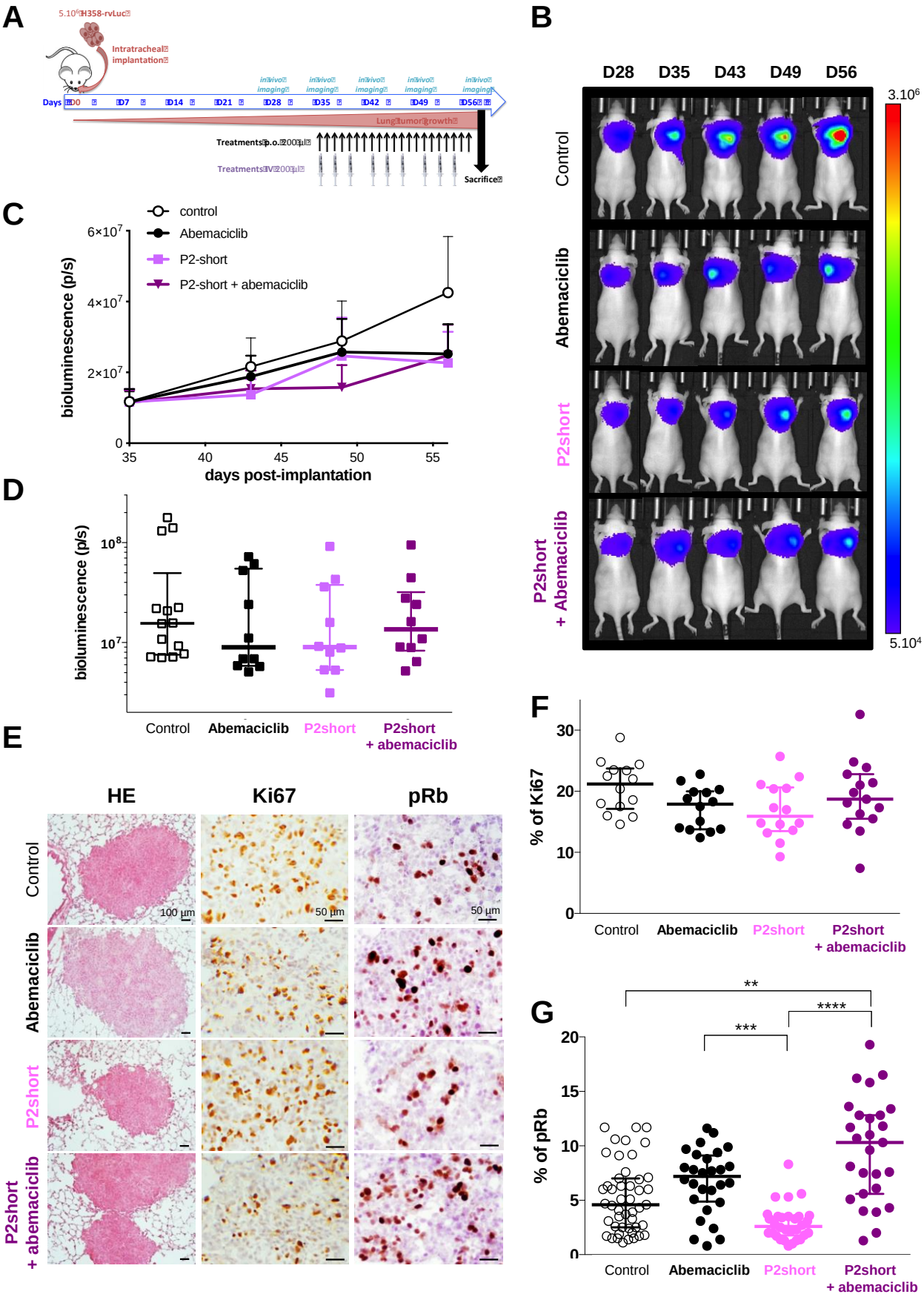
A
5.10⁶ H358-rvLuc
Intratracheal implantation
Days
D0
D7
D14
D21
D28
D35
D42
D49
D56
in vivo imaging
Lung tumor growth
Treatments p.o. 200µl
Treatments IV 200µl
Sacrifice
B
D28
D35
D43
D49
D56
Control
Abemaciclib
P2short
P2short + Abemaciclib
3.10⁶
5.10⁴
C
control
Abemaciclib
P2-short
P2-short + abemaciclib
bioluminescence (p/s)
6×10⁷
4×10⁷
2×10⁷
0
35
40
45
50
55
days post-implantation
D
bioluminescence (p/s)
10⁸
10⁷
Control
Abemaciclib
P2short
P2short + abemaciclib
E
HE
Ki67
pRb
Control
Abemaciclib
P2short
P2short + abemaciclib
100 µm
50 µm
50 µm
F
% of Ki67
30
20
10
0
Control
Abemaciclib
P2short
P2short + abemaciclib
G
**
***
****
% of pRb
20
15
10
5
0
Control
Abemaciclib
P2short
P2short + abemaciclib

**FIGURE S5 – Effect of P2shortA and Abemaciclib in orthotopic H358 tumour-bearing mice following intravenous injection**

**(A)** Schematic representation of H358 orthotopic tumours growth and of the treatments plan. The mice were inoculated with H358-rvLuc cells and randomized after 5 weeks into 3 groups of 10 mice and one control group of 14 mice. Vehicle or Abemaciclib 10 $mg.kg^{-1}$ were administered *per os* every days for 3 weeks. 0.9 $mg.kg^{-1}$ P2shortA was injected intravenously 3 times a week for 3 weeks. **(B)** Overtime thoracic bioluminescence images of H358-Luc tumours. One representative mouse (dorsal view) per group is shown. **(C)** Treatments with abemaciclib and/or P2shortA trend to inhibit the growth of orthotopic H358 tumours. The results are expressed as the mean ± SEM (control group, n=14; treated groups, n=10). **(D)** Thoracic bioluminescence level in each mouse at day 56. Bars, medians with interquartiles. **(E)** Histological (HE) and immunohistochemistry for Ki67 and phosphorylated-Rb (pRb) on lung tumour sections. Scale bars, 100 µm (HE) and 50 µm (Ki67 and pRb). **(F)** Ki67-positive cells were quantified on different fields (2-8) in three or four mice per group, and reported as % Ki67 positive cells. Bars, medians with interquartiles. **(G)** pRb-positive cells were quantified on different fields (2-29) in three or four mice per group, and reported as % pRb positive cells. Bars, medians with interquartiles. Kruskall-Wallis test with Dunn's multiple comparisons *posthoc* tests ($p < 0.0001$); **, treatment combination group compared to control group; ***, abemaciclib group compared to P2shortA group; ****, treatment combination group compared to P2shortA group.

## Figure S6

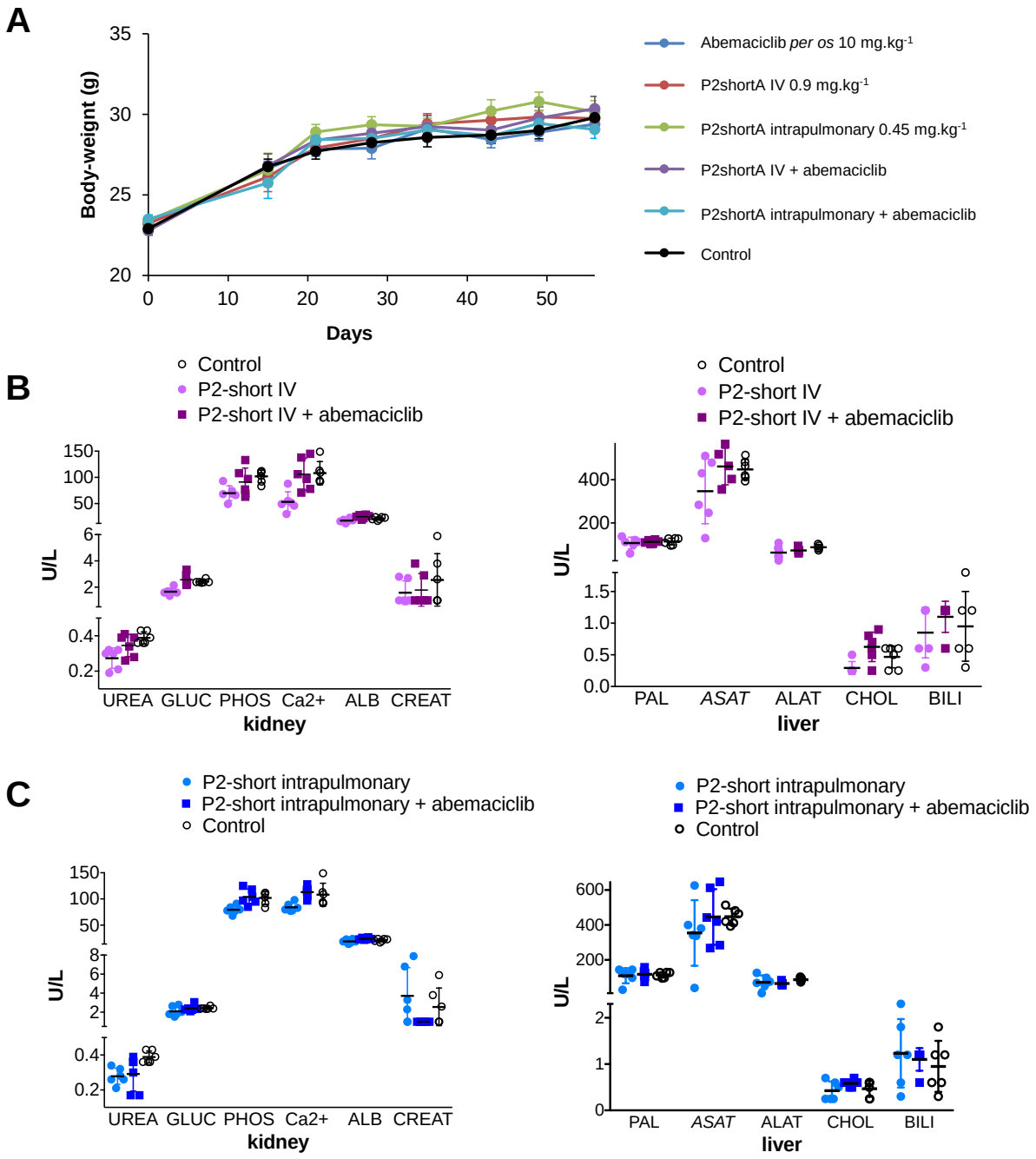


**FIGURE S6 – P2shortA and Abemaciclib treatments were well-tolerated in mice with orthotopic H358 lung tumour.**

**(A)** Mice body-weight in each group from the tumour implantation to sacrifice at day 56. Treatments began at day 35 (means ± SD; control, n=14; treated groups, n=10). **(B-C)** Plasma biochemical values of mice after intravenous (**B**) or intrapulmonary (**C**) administration of P2shortA were assessed. Data represent the means ± SD of 6 mice per group. UREA: blood urea nitrogen; GLUC, glucose; PHOS, phosphorus; Ca2+, calcium; ALB, albumin; CREAT, creatinine; PAL, alkaline phosphatase; ASAT, aspartate amino-transferase; ALAT, alanine amino-transferase; CHOL, cholesterol, BILI, bilirubin.

**Table S1.** Clinical and biological characteristics of patients according to the histological subtype.

| | **All patients** n=215 n (%) | **ADC** n=111 n (%) | **SCC** n=104 n (%) | *p* value |
|---|---|---|---|---|
| **Gender** | | | | |
| Male | 161 (75%) | 71 (64%) | 90 (88%) | 0.0001 |
| Female | 54 (25%) | 40 (36%) | 14 (12%) | |
| **Age**, Median (range) | 61.2 (47-70) | 64 (40-82) | 67.5 (41-85) | |
| **Smoking status** | | | | |
| Current smokers | 102 (48%) | 56 (50%) | 46 (44%) | 0.0069 |
| Former smokers | 95 (44%) | 40 (36%) | 55 (53%) | |
| Passive smokers | 2 (1%) | 1 (1%) | 1 (1%) | |
| Non -smokers | 16 (7%) | 14 (13%) | 2 (2%) | |
| Professional exposures | 50 (23%) | 25 (23%) | 25 (24%) | |
| **Stage** | n=211 | n=108 | n=103 | 0.02 |
| I | 79 (38%) | 42 (39%) | 37 (36%) | |
| II | 57 (27%) | 24 (22%) | 33 (32%) | |
| III | 60 (28%) | 29 (27%) | 31 (30%) | |
| IV | 15 (7%) | 13 (12%) | 2 (2%) | |
| ***EGFR* mutation*** | n=112 | n=109 | n=3 | 1.00 |
| No mutation | 100 (89%) | 97 (89%) | 3 (100%) | |
| Mutation (exons 18-21) | 12 (11%)[#] | 12 (11%) | 0 | |
| ***KRAS* mutation*** | n=112 | n=108 | n=4 | 0.30 |
| No mutation | 73 (65%) | 69 (64%) | 4 (100%) | |
| Mutation (exon 2) | 39 (35%) | 39 (36%) | 0 | |
| ***HER2* mutation*** | n=86 | n=85 | n=1 | 1.00 |
| No mutation | 83 (97%) | 82 (96%) | 1 (100%) | |
| Mutation | 3 (3%) | 3 (4%) | 0 | |
| ***PI3KCA* mutation*** | n=30 | n=30 | n=0 | |
| No mutation | 30 (100%) | 30 (100%) | | |
| Mutation | 0 | 0 | | |
| **BRAF mutation*** | n=89 | n=86 | n=3 | 0.13 |
| No mutation | 85 (96%) | 83 (97%) | 2 (67%) | |
| Mutation | 4 (4%) | 3 (3%) | 1 (33%) | |
| ***FGFR1* amplification**** | n=5 | n=0 | n=5 | |
| No amplification | 5 (100%) | 0 | 5 (100%) | |
| Amplification | 0 | 0 | 0 | |
| ***ALK* rearrangement**** | n=66 | n=64 | n=2 | 1.00 |
| Negative | 66 (100%) | 64 (100%) | 2 (100%) | |
| Positive | 0 | 0 | 0 | |
| ***ROS1* rearrangement**** | n=30 | n=27 | n=3 | 1.00 |
| Negative | 29 (97%) | 26 (96%) | 3 (100%) | |
| Positive | 1 (3%) | 1 (4%) | 0 | |
| ***CMET* amplification**** | n=11 | n=8 | n=3 | 1.00 |
| Negative | 10 (91%) | 7 (88%) | 3 (100%) | |
| Positive | 1 (9%) | 1 (12%) | 0 | |
| **Cyclin D1 expression** | n=206 | n=107 | n=99 | <0.0001 |
| 0-10% | 87 (42%) | 24 (22%) | 63 (64%) | |
| >10% | 119 (58%) | 83 (78%) | 36 (36%) | |
| **CDK4 expression** | n=215 | n=111 | n=104 | 0.67 |
| 0-10% | 81 (38%) | 40 (36%) | 41 (39%) | |
| >10% | 134 (62%) | 71 (64%) | 63 (61%) | |
| **pRb expression** | n=215 | n=111 | n=104 | 0.0003 |
| 0-10% | 166 (77%) | 97 (87%) | 69 (66%) | |
| >10% | 49 (23%) | 14 (13%) | 35 (34%) | |

*Mutations were detected by next- generation sequencing (NGS). **Rearrangements and amplifications were detected by immunohistochemistry and/or fluorescent in situ hybridization (FISH). Statistical analysis was

performed using Fisher's exact test. Missing data were excluded from the analysis. #One mutation of exon 18, five deletions of exon 19, one mutation of exon 20, and five substitution of exon 21 L858R.

**Table S2:** immunohistochemical and molecular characterization of NSCLC tumours

| | | Cyclin D1 expression | | | | CDK4 expression | | | | pRb expression | |
|---|---|---|---|---|---|---|---|---|---|---|---|
| | **All patients** | **0-10%** | **>10%** | | **All patients** | **0-10%** | **>10%** | | **0-10%** | **>10%** | |
| | n (%) | n=87<br>n (%) | n=119<br>n (%) | *p* value | n (%) | n=81<br>n (%) | n=134<br>n (%) | *p* value | n=166<br>n (%) | n=49<br>n (%) | *p* value |
| **Cyclin D1 expression** | n=206 | | | | n=206 | | | 0.0001 | | | 0.9 |
| 0-10% | 87 (42%) | | | | 87 (42%) | 47 (54%) | 40 (46%) | | 66 (76%) | 21 (34%) | |
| >10% | 119 (58%) | | | | 119 (58%) | 29 (24%) | 90 (76%) | | 91 (76%) | 28 (24%) | |
| **CDK4 expression** | n=206 | | | 0.0001 | n=215 | | | | | | |
| 0-10% | 76 (37%) | 47 (54%) | 29 (24%) | | 81 (38%) | | | | 72 (89%) | 9 (11%) | 0.0014 |
| >10% | 130 (63%) | 40 (46%) | 90 (76%) | | 134 (62%) | | | | 94 (70%) | 40 (30%) | |
| **pRb expression** | n=206 | | | 0.9 | n=215 | | | 0.0014 | | | |
| 0-10% | 157 (76%) | 66 (76%) | 91 (76%) | | 166 (77%) | 72 (89%) | 94 (70%) | | | | |
| >10% | 49 (24%) | 21 (34%) | 28 (24%) | | 49 (23%) | 9 (11%) | 40 (30%) | | | | |
| ***EGFR*** | n=108 | n=26 | n=82 | 1.00 | n=112 | n=41 | n=71 | 0.53 | n=96 | n=16 | 0.20 |
| No mutation | 97 (90%) | 24 (72%) | 73 (89%) | | 100 (89%) | 38 (93%) | 62 (87%) | | 84 (88%) | 16 (100%) | |
| Mutation [a] | 11 (10%) | 2 (8%) | 9 (11%) | | 12 (11%) | 3 (7%) | 9 (13%) | | 12 (12%) | 0 | |
| ***KRAS*** | n=107 | n=26 | n=81 | | n=112 | n=41 | n=71 | | n=97 | n=15 | |
| No mutation | 69 (64%) | 22 (85%) | 47 (58%) | 0.0178 | 73 (65%) | 25 (61%) | 48 (68%) | 0.53 | 62 (64%) | 11 (73%) | 0.57 |
| Mutation [b] | 38 (36%) | 4 (15%) | 34 (42%) | | 39 (35%) | 16 (39%) | 23 (32%) | | 35 (36%) | 4 (27%) | |
| ***HER2*** | n=81 | n=19 | n=62 | 1.00 | n=83 | n=30 | n=53 | 1.00 | n=73 | n=10 | 0.32 |
| No mutation | 78 (96%) | 19 (100%) | 59 (95%) | | 80 (96%) | 29 (97%) | 51 (96%) | | 71 (97%) | 9 (90%) | |
| Mutation | 3 (4%) | 0 | 3 (5%) | | 3 (4%) | 1 (3%) | 2 (4%) | | 2 (3%) | 1 (10%) | |
| ***PI3KCA*** | n=28 | n=7 | n=21 | | n=31 | n=9 | n=22 | | n=28 | n=3 | |
| No mutation | 28 (100%) | 7 (100%) | 21 (100%) | | 31 (100%) | 9 (100%) | 22 (100%) | | 28 (100%) | 3 (100%) | |
| Mutation | 0 | 0 | 0 | | 0 | 0 | 0 | | 0 | 0 | |
| ***BRAF*** | n=85 | n=20 | n=65 | 1.00 | n=88 | n=32 | n=56 | 0.0154 | n=77 | n=11 | 1.00 |
| No mutation | 83 (98%) | 20 (100%) | 63 (97%) | | 84 (95%) | 28 (88%) | 56 (100%) | | 73 (95%) | 11 (100%) | |
| Mutation | 2 (2%) | 0 | 2 (3%) | | 4 (5%) | 4 (12%) | 0 | | 4 (5%) | 0 | |
| ***FGFR1*** | n=5 | n=2 | n=3 | | n=5 | n=1 | n=4 | | n=4 | n=1 | |
| No amplification | 5 (100%) | 2 (100%) | 3 (100%) | | 5 (100%) | 1 (100%) | 4 (100%) | | 4 (100%) | 1 (100%) | |
| Amplification | 0 | 0 | 0 | | 0 | 0 | 0 | | 0 | 0 | |
| ***ALK*** [c] | n=62 | n=10 | n=52 | | n=66 | n=18 | n=48 | | n=61 | n=5 | |
| Negative | 62 (100%) | 10 (100%) | 52 (100%) | | 66 (100%) | 18 (100%) | 48 (100%) | | 61 (100%) | 5 (100%) | |
| Positive | 0 | 0 | 0 | | 0 | 0 | 0 | | 0 | 0 | |
| ***ROS1*** [c] | n=29 | n=2 | n=27 | 1.00 | n=30 | n=7 | n=23 | 1.00 | n=29 | n=1 | 1.00 |
| Negative | 28 (97%) | 2 (100%) | 26 (96%) | | 29 (97%) | 7 (100%) | 22 (96%) | | 28 (97%) | 1 (100%) | |
| Positive | 1 (3%) | 0 | 1 (4%) | | 1 (3%) | 0 | 1 (4%) | | 1 (3%) | 0 | |
| ***CMET*** | n=10 | n=1 | n=9 | 1.00 | n=11 | n=3 | n=8 | 1.00 | n=11 | n=0 | 1.00 |
| No amplification | 9 (90%) | 1 (100%) | 8 (89%) | | 10 (91%) | 3 (100%) | 7 (88%) | | 10 (91%) | 0 | |
| Amplification | 1 (10%) | 0 | 1 (11%) | | 1 (9%) | 0 | 1 (12%) | | 1 (9%) | 0 | |

Missing data were excluded from the analysis. [a] exons 18-21; [b] exon 2; [c] rearrangement. Statistical analysis was performed using Fisher's exact test